Collider Phenomenology of Non-Minimal Universal Extra Dimensional Model at 13 TeV

Avnish

Institute of Physics, Bhubaneswar

12.03.2021

Outlines:

Motivation

Dimension compactification and Orbifolding

Non-minimal Universnal Extra Dimensional Model

Kaluza Klein decomposition

Mass and Coupling Modification in nmUED

Collider Phenomenology at the LHC

Conclusion

- The Standard Madel(SM) is the best phenomenological model till present to explain interactions of fundamental particles at high energy.
- The SM explains the most of the observed phenomenon but not all of them.
- The SM niether have dark matter particle and nor have right handed neutrinos to explain experimentally stablised findings.
- It naturally demands to explore beyond the SM physics.
- UED is one of the avenues to address this, which is mainly motivated by hierarchy issues and it additionally provide candidates of dark matter.
- Minimal UED is excluded by collider searches. This motivates us to explore non-minimal UED scenario at colliders.

arXive: 2012.15137

Dimension compactification and Orbifolding

- UED is an extension of the 1 + 3 dimensional Minkowski world $\mathbb{M}_4$ to a 1 + 4 dimensional $\mathbb{M}_4 \times \mathbb{S}_1$ world. The metric convention is g_{MN}= diag$(+,-,-,-,-)$.
- The fourth spatial dimension corresponds to a topology of a circle $\mathbb{S}_1$ with a radius R implying that the extra dimension is compact.
- Compactification means the physical identification of the points y and y + 2πR along the extra dimension y which suggests for any field, viz.$\Phi \Rightarrow \Phi(y) = \Phi(y + 2\pi R)$.
- Eventually, any function of spacetime which has a periodic boundary condition along a spatial dimension, we can expand it in modes, here in so called Kaluza-Klein Modes.
- Due to compactification, chirality operator can't be defined at odd modes, so no chiral fermions.
- TASI 2006 Lectures on Extra Dimensions by Kaustubh Agashe

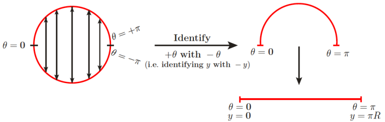

- It can be solved by mapping compactification not on a circle, but on a line segment imposing suitable boundary conditions to the bulk fields(i.e. line segment $0 < y < l$).
- Physically, it is $\mathbb{S}_1/Z_2$ orbifold as depicted in figure. We can relate l to a compactification radius R by $l = \pi R$.

KK-Parity

- Orbifolding breaks the translational invariance of extra spatial dimension and hence the fifth dimensional momentum is no more a conserved quantity.
- There remains an additional symmetry, an discrete symmetry, called KK-parity.
- KK-parity conservation can be manifested as the translational symmetry: $y \rightarrow y - \pi R$.
- For nth KK level particle, KK-parity is $(-1)^n$.
- All the Standard Model fields are of even KK-parity.
- Conservation of KK-parity have great implication:
- The lightest level-one KK-mode particle (LKP) is stable and only pair production is allowed for odd level KK-modes.
- All direct couplings of the SM particles to even number KK states are loop suppressed and can occur through brane-localized interactions.
- Generally, in the minimal UED, KK-parity remains a good symmetry and remains unbroken so long as no explicit KK-parity violating interactions are introduced at the orbifold fixed points.

Non-minimal Universnal Extra Dimensional Model

The action is invariant under the gauge symmetry of the standard model $SU(3)_C \times SU(2)_L \times U(1)_Y$ in **5 D** (five dimensions).
The actions of all three gauge sectors look like:

$$S_{\mathrm{G}} = \int d^4x \int_0^{\pi R} dy \left\{ -\frac{1}{4} G^a_{MN} G^{aMN} + \Big(\delta(y) + \delta(y - \pi R)\Big) \left[-\frac{r_G}{4} G^a_{\mu\nu} G^{a\mu\nu} \right] \right\},$$

$$S_{\mathrm{W}} = \int d^4x \int_0^{\pi R} dy \left\{ -\frac{1}{4} W^i_{MN} W^{iMN} + \Big(\delta(y) + \delta(y - \pi R)\Big) \left[-\frac{r_W}{4} W^i_{\mu\nu} W^{i\mu\nu} \right] \right\},$$

$$S_{\mathrm{B}} = \int d^4x \int_0^{\pi R} dy \left\{ -\frac{1}{4} B_{MN} B^{MN} + \Big(\delta(y) + \delta(y - \pi R)\Big) \left[-\frac{r_B}{4} B_{\mu\nu} B^{\mu\nu} \right] \right\},$$

- The action consists of two parts. First,the usual gauge kinetic term in **5 D**. The second part is the Brane (also called Boundary) localized kinetic terms (BLKT).
- These terms appear only at the boundaries of the brane and the bulk as can be seen by the delta function over extra dimension.
- r_G, r_W and r_B are the BLKT parameters corresponding to the gluon, W_μ and B_μ fields.
- The dimension of the brane-bulk boundary is less than the actual dimension of the theory by unity. Therefore, the BLKTs are written in **4 D** as can be noted by the greek indices attached to the fields.

The fermionic field content of the model:

$SU(2)$ representations	SM mode	KK modes
Quark doublet	$Q_L = \begin{pmatrix} u_L \\ d_L \end{pmatrix}$	$Q_L^{(n)} = \begin{pmatrix} U_L^{(n)} \\ D_L^{(n)} \end{pmatrix}$, $Q_R^{(n)} = \begin{pmatrix} U_R^{(n)} \\ D_R^{(n)} \end{pmatrix}$
Lepton doublet	$L_L = \begin{pmatrix} \nu_L \\ e_L \end{pmatrix}$	$L_L^{(n)} = \begin{pmatrix} \nu_L^{(n)} \\ e_L^{(n)} \end{pmatrix}$, $L_R^{(n)} = \begin{pmatrix} \nu_R^{(n)} \\ e_R^{(n)} \end{pmatrix}$
Quark Singlet	u_R	$u_R^{(n)}, u_L^{(n)}$
Quark Singlet	d_R	$d_R^{(n)}, d_L^{(n)}$
Lepton Singlet	e_R	$e_R^{(n)}, e_L^{(n)}$

$$S_{\text{fermion}} = \int d^4x \int_0^{\pi R} dy \sum_{i=1}^{3} \Big\{ i\overline{Q}_i \Gamma^M \mathcal{D}_M Q_i + r_f \Big(\delta(y) + \delta(y - \pi R)\Big) \Big[i\overline{Q}_i \gamma^\mu \mathcal{D}_\mu P_L Q_i \Big]$$

$$+ i\overline{L}_i \Gamma^M \mathcal{D}_M L_i + r_f \Big(\delta(y) + \delta(y - \pi R)\Big) \Big[i\overline{L}_i \gamma^\mu \mathcal{D}_\mu P_L L_i \Big] \Big\}$$

$+$ similar terms for the right handed fields

- Here $i = 1, 2, 3$ is the generation index, $\Gamma_M = (\gamma_\mu, i\gamma_5)$ denotes γ matrices in **5 D**. $\mathcal{D}_M$ is the **5 D** covariant derivative.
- r_f is the BLKT parameter for the left as well as right chiral quark fields. One can also consider r_Q and r_L for quarks and leptons, separately.

The scalar sector of the model :

$$S_{\text{scalar}} = \int d^4x \int_0^{\pi R} dy \Big\{ (\mathcal{D}^M\Phi)^\dagger(\mathcal{D}_M\Phi) + \mu_5^2\Phi^\dagger\Phi - \lambda_5(\Phi^\dagger\Phi)^2 \\ + \Big(\delta(y) + \delta(y-\pi R)\Big)\Big[r_\Phi(\mathcal{D}^\mu\Phi)^\dagger(\mathcal{D}_\mu\Phi) + \mu_B^2\Phi^\dagger\Phi - \lambda_B(\Phi^\dagger\Phi)^2 \Big] \Big\}$$

- To get a flat (i.e. y independent) Higgs profile, these parameters are required to be connected as $\mu_B^2 = r_\Phi \mu_5^2$ and $\lambda_B = r_\Phi \lambda_5$.

- The entire Electro-Weak gauge sector and the scalar sector produce a very intriguing scenario. Masses of the KK $W_\mu^{(n)}$, $B_\mu^{(n)}$ bosons depend on the BLKT parameters r_W and r_B, respectively.

- Since the mass term of massive Electro-Weak gauge bosons appear after the breaking of Electro-Weak symmetry by the VEV of the Higgs, the role of r_Φ also become crucial in determining the masses of the KK electroweak gauge bosons.

KK decomposition

- All the actions written above contain the informations of the full theory in **5 D**.
- We have to come down to a **4 D** effective theory because the SM is a **4 D** theory.
- We expand **5 D** fields into x_μ and y dependent wave functions and select the form of the y dependent wave functions from appropriate boundary conditions which weeds out extra degrees of freedom that are not part of the SM.
- These mode expansions are fed into the actions and on integrating out the extra dimensional degree of freedom (y), we obtain mass determining transcendental equations, terms encoding level-mixing and coupling factors.

$$G_\mu^{a(n)}(x,y) = \sum_{n=0}^{\infty} G_\mu^{a(n)}(x)\ f_G^{(n)}(y).$$

- After matching appropriate boundary condition, we determine the y dependent form to be :

$$f_G^{(n)}(y) = N_G^{(n)} \times \begin{cases} \dfrac{\cos(M_G^{(n)} y)}{C_G} & \text{for even } n \\ -\dfrac{\sin(M_G^{(n)} y)}{S_G} & \text{for odd } n \end{cases},$$

$$C_G = \cos\left(\frac{M_G^{(n)}\pi R}{2}\right), \quad S_G = \sin\left(\frac{M_G^{(n)}\pi R}{2}\right).$$

♦ The transcendental equations to determine nth level Gluon mass $M_G^{(n)}$:

$$r_G M_G^{(n)} = \begin{cases} -2\tan\left(\frac{M_G^{(n)}\pi R}{2}\right) & \text{for } n \text{ even} \\ 2\cot\left(\frac{M_G^{(n)}\pi R}{2}\right) & \text{for } n \text{ odd} \end{cases} .$$

♦ These transcendental equations are very important in nmUED as they provide the KK masses of particles whose boundary terms have been included in the theory.

♦ $N_G^{(n)}$ are the normalization of the wave function determined from the boundary conditions.

$$N_G^{(n)} = \left[\left(\frac{\pi R}{2}\right)\left(1 + \frac{r_G^2 {M_G^{(n)}}^2}{4} + \frac{r_G}{\pi R}\right)\right]^{-\frac{1}{2}}$$

Mass terms of charged and neutral EW gauge bosons

- We see, after the KK decomposition of the $W_M = (W_\mu, W_5)$ boson, its charged bosons are:

$$W_\mu^{\pm(n)}(x,y) = W_\mu^{\pm(n)}(x)\ f_W^{(n)}(y), \quad W_5^{\pm(n)}(x,y) = W_5^{\pm(n)}(x) f_{\tilde{W}}^{(n)}(y)$$

- Same also holds for the $U(1)_Y$ gauge boson B_M. There are two sources of masses:
- First, the KK mass which comes from the solution of the similar transcendental equation as given above by replacing r_G by r_W i.e. the corresponding BLKT parameter for the W boson.
- Second, the mass term from the Electro-Weak symmetry breaking comes from the boundary term in action of Higgs after Higgs getting VEV.
- Inserting the KK expansions of W boson as written above in the Lagrangian, we obtain:

$$\mathcal{L}_{W(\mathrm{vev})} = M_W^2 \left(\frac{r_W + \pi R}{r_\Phi + \pi R} \right) \mathcal{I}_A^{nm}\ W^{\mu(n)-}(x) W_\mu^{(m)+}(x)$$

$$\mathcal{I}_A^{nm} = \int_0^{\pi R} dy \left[1 + r_\Phi \Big(\delta(y) + \delta(y - \pi R) \Big) \right] f_W^{(n)}(y) f_W^{(m)}(y)$$

- $\mathcal{I}_A^{nm}$ is called the overlap integral.

♦ After collecting all the relevant mass terms of charged $W^{(n)\pm}$:

$$\mathcal{L}^{W^{\mu(n)\pm}}(\text{mass}) = \left(\left(\frac{r_W + \pi R}{r_\Phi + \pi R}\right)\mathcal{I}_A^{nm} M_W^2 + M_{W,n}^2\right)\; W^{\mu(n)-}(x)W_\mu^{(n)+}(x)$$
$$= M_W^{(n)2} W^{\mu(n)-}(x)W_\mu^{(n)+}(x).$$

♦ In this expression, $M_{W,n}$ denotes the solution of transcendental equation for W boson and $M_W^{(n)}$ is the final mass of KK $W_\mu^{(n)+}$ boson.

♦ Mixing between gauge boson:

$$\int (D_\mu\Phi)^\dagger(D^\mu\Phi)dy \Rightarrow \frac{v^2}{8}\Big[g^2\mathcal{I}_{\phi_{WW}} W^{\mu 3(n)}W_\mu^{3(m)} - 2gg'\mathcal{I}_{\phi_{WB}} W^{\mu 3(n)}B_\mu^{(m)} + {g'}^2\mathcal{I}_{\phi_{BB}} B^{\mu(n)}B_\mu^{(m)}\Big]$$

$$\mathcal{I}_{\phi_{WW}} = \int dy[1 + r_\phi\{\delta(y) + \delta(y-\pi R)\}]\frac{(r_W + \pi R)}{(r_\phi + \pi R)} f_W^{(n)} f_W^{(m)},$$
$$\mathcal{I}_{\phi_{BB}} = \int dy[1 + r_\phi\{\delta(y) + \delta(y-\pi R)\}]\frac{(r_B + \pi R)}{(r_\phi + \pi R)} f_B^{(n)} f_B^{(m)},$$
$$\mathcal{I}_{\phi_{WB}} = \int dy[1 + r_\phi\{\delta(y) + \delta(y-\pi R)\}]\sqrt{r_B + \pi R}\,\frac{\sqrt{r_W + \pi R}}{(r_\phi + \pi R)} f_W^{(n)} f_B^{(m)}.$$

- $W^{\mu 3}$ and B^{μ} can be written in terms of mass eigenstates as:

$$W^{\mu 3} = c_1 W^{\mu 3\prime} + c_2 B^{\mu\prime}, \quad B^{\mu} = c_2 W^{\mu 3\prime} + c_1 B^{\mu\prime}, \quad c_1^2 + c_2^2 = 1$$

- Interesting phenomenon of level-mixing happens due to the presence of large boundary terms. It is the mixing between different KK levels of same state.
- This KK number violating phenomenon is theoretically possible as the translational invariance in 5D is broken by the fixed points at the boundaries.
- KK parity conservation would restrict such mixing limited within even and odd states separately.
- In the quark sector, such level-mixing appears if we allow boundary-localized Yukawa terms (BLYT), denoted by r_Y.
- For the lighter first two generations, the mixing is usually negligible (although there is apparently no reason forces such assumption as the boundary terms are completely free parameters on their own and bears no imprint of SM physics).
- But the phenomenology for the top quark could be quite different. However, we do not explore this here.

Implications of BLKTs

- In minimal UED, the mixing between $B_\mu^{(1)}$ and $W_\mu^{3(1)}$ is nominal and hence, the level-1 Weinberg angle can well be considered negligible (zero).
- The boundary localized terms also modify the KK mode wave functions of the Electro-Weak gauge bosons, apart from modifying the KK mass spectra. This makes non-zero Weinberg angle for all KK levels and results in significant mixing between $B_\mu^{(n)}$ and $W_\mu^{3(n)}$. This fact, in turn, has important implications for the dark matter phenomenology.
- We may have the LKP other than the usual level-1 KK Photon ($\gamma^{(1)}$) due to the interplay of Electro-Weak gauge and scalar BLKT parameters.
- The LKP may well be a mixture of $SU(2)_L$ and $U(1)_Y$ gauge components with the mixing angles controlled by r_W, r_B, r_Φ.
- Interestingly, due to the modifications in KK mode wave functions, the interaction vertices amongst the Electro-Weak gauge bosons and the fermions also get modified.
- These modifications comes from the overlap integrals of wave functions which are now governed by various BLKT parameters.

Coupling Modification Factor

- One of the novel features of nmUED scenario is the modification in various interaction vertices.
- This modification appears once we plug in the KK expansion in **5 D** lagrangian and integrate out the extra dimensional degrees of freedom y.
- To illustrate, $\Psi^{(k)} - V_\mu^{(l)} - \Psi^{(m)}$ interaction where we denote a generic fermion field and a gauge boson by Ψ and V_μ, respectively.

$$\tilde{g} \int d^4x \int dy \sum_{k,l,m} \left(\Psi^{(k)}(x)\ \tilde{f}_\Psi^{(k)}(y)\right) \times \left(V_\mu^{\pm(l)}(x)\ f_V^{(l)}(y)\right) \times \left(\Psi^{(m)}(x)\ \tilde{f}_\Psi^{(m)}(y)\right)$$

- The SM interaction involving all the zero mode excitations can be reproduced if we consider the all KK indices to be zero.
- Therefore, **5 D** gauge coupling $\tilde{g}$ multiplied by the overlap integral factor with KK numbers $k = l = m = 0$ gives the SM coupling:

$$g = \frac{\tilde{g}}{\sqrt{r_V + \pi R}}$$

- where r_V is BLKT parameter corresponding to $V_M^{(n)}$.
- The proper normalization of the fields are essential for this correspondance between **5 D** coupling and its SM counterpart.

- As for the interaction involving KK level, we are allowed to pick only those mode numbers which satisfy a general selection rule fixed by the conservation of KK number. For example, the coupling which is important for pair production of KK quark-antiquark, is $Q^{(0)} - V^{(1)} - Q^{(1)}$, where $V^{(1)}$ signifies any level-1 gauge boson.
- In mUED, this coupling is exactly same as in the SM as the y integral of KK mode functions becomes unity.
- However, due to the presence of BLKTs, the y profile of KK excitations differ from the usual mUED case, giving rise to non-trivial overlap integral.
- The overlap integral factor has a complicated dependance on the BLT parameters through the nomalization factors etc.

- These factors may deviate from unity and thus, can enhance or reduce the particular couplings and hence can affect collider phenomenology significantly, specially the interaction vertex $Q^{(0)} - V^{(1)} - Q^{(1)}$.
- We can see it for interaction vertex $Q^{(0)} - G^{(1)} - Q^{(1)}$ coupling modification factor $\Rightarrow$
- We use customary notation $R_G = \frac{r_G}{R}$ everywhere.

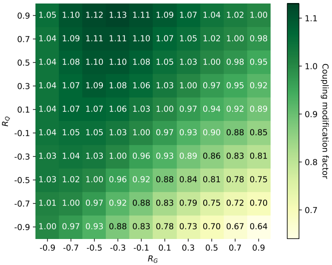

Collider Phenomenology of nmUED

- The dominant channels of production of level 1 KK particles for our study are : $G^{(1)}G^{(1)}$, $Q^{(1)}\overline{Q^{(1)}}$, $G^{(1)}Q^{(1)}$, $G^{(1)}\overline{Q^{(1)}}/q^{(1)}$, $q^{(1)}\overline{q^{(1)}}$, $q^{(1)}q^{(1)}$
- After production at the LHC, these KK particles decay to LKP and other SM particles giving multi-jet high missing energy collider signatures.
- R^{-1} sets the overall scale over which r_G, r_Q fix the masses of the KK gluon and KK quarks respectively.
- BLKT also control dynamics as the coupling between level 1 KK gluons and level 1 KK quark and a SM quark and gluon apppear in t-channel diagrams of pair production of KK quark and KK gluon.
- Mass hierarchy among level 1 KK particles affects the decay of level 1 KK particles and decide final products.
- We considered both hierarchy: $R_G > R_Q$ and $R_G < R_Q$.
- $R_G < R_Q$ would render a more massive KK gluon than KK quarks and $R_G > R_Q$ would do the opposite.

- With $M_{G^{(1)}} > M_{Q^{(1)}}$, the level 1 KK gluon decays primarily to the set of a SM quark and its level 1 KK quark counterpart.
- With $R_Q < R_W < R_B$, the level 1 KK quarks decay to a SM quark and a $W^{(1)\pm}/Z^{(1)}/\gamma^{(1)}$.
- The only decay mode open for $W^{(1)\pm}$ is $W^{\pm}\gamma^{(1)}$.
- A more interesting situation arises for the case of $M_{G^{(1)}} < M_{Q^{(1)}}$ where a level 1 KK gluon decays into three body final state comprising q - $\bar{q}$ - $Z^{(1)}/\gamma^{(1)}$ and q - $\bar{q}'$ - $W^{(1)\pm}$.
- This study is focused onto strong production and the resulting multi-jet channel.
- We do not intend to discuss the Electro-Weak sector in detail, but only make necessary arrangenements just suitable for the ATLAS analysis.
- Having blocked the arrival of leptons from the decay of KK particles, we veto any leptons coming from $W^{\pm}$ as well targeting the ATLAS results [ATLAS-conf-2019-040].

- The dominant channel is $gg \to G^{(1)}G^{(1)}$ with $G^{(1)}$ in t(u)-channel.
- The sub-dominant channels are $q\bar{q} \to G^{(1)}G^{(1)}$ with a $Q^{(1)}$ in t(u)-channel.
- The s-channel g exchange diagram and t(u)-channel $Q^{(1)}$ exchange diagram of $q\bar{q} \to G^{(1)}G^{(1)}$ interfere distructively.
- Mass of level 1 KK gluon kept fix at 2 TeV by varying $\mathrm{R_G}$ and R^{-1}.
- $\mathrm{R_Q}$ has also varied to change the mass of level 1 KK quark and the coupling modification factor of $G^{(1)}$-$Q^{(1)}$-Q.
- Negative values of $\mathrm{R_G}$ allow smaller R^{-1} and as $\mathrm{R_G}$ increase we need larger R^{-1} to keep mass fixed.
- From (low $\mathrm{R_G}$, low $\mathrm{R_Q}$) region, cross section increases for increasing $\mathrm{R_Q}$ for fixed $\mathrm{R_G}$ (hence, fixed R^{-1}) towards (low $\mathrm{R_G}$, high $\mathrm{R_Q}$) region.
- As $\mathrm{R_Q}$ for fixed $\mathrm{R_G}$ (hence, fixed R^{-1}) increases here, it enhances the coupling modification factor.
- Also increasing $\mathrm{R_Q}$ for fixed R^{-1}, reduces the mass of level 1 KK quark which is in propagation.

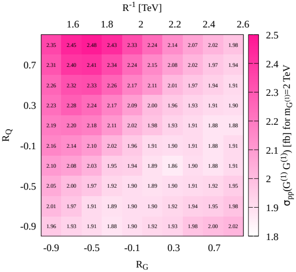

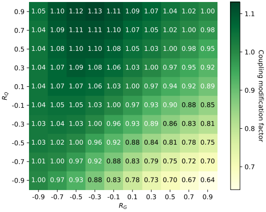

- At top, moving horizontally while keeping $\mathrm{R_Q}$ fixed, cross- section reduces.
- As $\mathrm{R_G}$ increases, it demands large R^{-1} to keep mass of level 1 KK gluon fixed.
- This large R^{-1} makes propagating KK quarks more massive, hence increasing propagation suppression.
- Additionally, the coupling modification factor is also decreasing.
- We have seen how a physical observable cross-section depends upon the parameters of the theory.

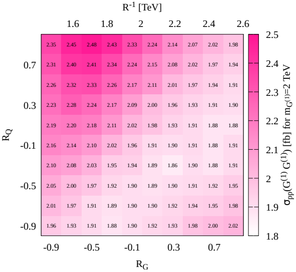

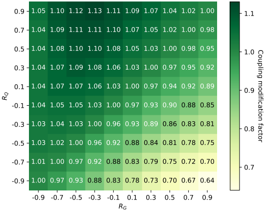

- At the LHC, this is a quark-gluon initiated process with a exchange of $G^{(1)}/Q^{(1)}$ in the t(u) channel.
- Mass of level 1 KK gluon kept fix at 2 TeV by varying $\mathrm{R_G}$ and R^{-1} but mass of evel 1 KK quark is varying.
- Varying $\mathrm{R_Q}$ changes the mass of level 1 KK quark and the coupling modidification factor of $G^{(1)}$-$Q^{(1)}$-Q.
- Dominant variation in the total cross-section is due the varying final state level-1 KK quark.
- The varying coupling modification factor contributes to the varying cross-section but mildly.

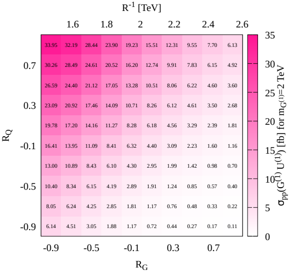

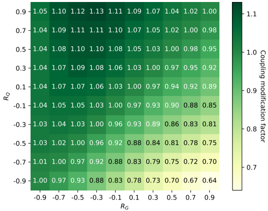

- Cross-section of pair produced level 1 KK quark-anti-quark (left) and quark -quark (right) have shown below.
- The dominant contribution ($pp \to U^{(1)}\bar{U}^{(1)}$) comes from quark-anti quark and gluon-gluon initiated processes.
- The dominant contribution ($pp \to U^{(1)}U^{(1)}$) comes from quark-quark fusion with exchange of a level-1 KK gluon in t(u) channel.
- The coupling modification factor and varying BLKT parameters show same effect on cross-section.
- These scans have been produced for fixed mass of 2 TeV of level 1 KK quark.

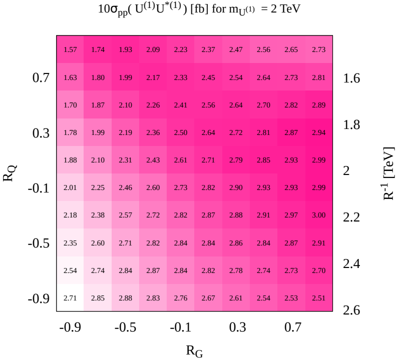

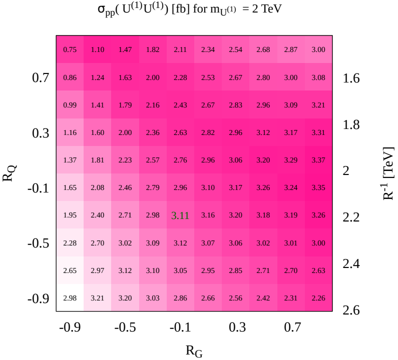

The ATLAS Search for High p_T Multi-jets

- We employed the ATLAS search [ATLAS-conf-2019-040] for high p_T multi-jet and large missing transverse momentum with no lepton in signal channel with total integrated luminosity of 139 fb^{-1} and the center of mass-energy $\sqrt{s} = 13$ TeV at the LHC for imposing detection bounds.
- To reconstruct events we closely followed it as far as possible.
- Signal channels classified according to their jet multiplicity (2-6) and effective mass ($\mathrm{m_{eff}}$).
- Jet-candidates have been reconstructed using $\mathrm{anti} - \mathrm{k_t}$ jet clustering algorithm with a jet radius parameter of 0.4 starting from the clusters of calorimeter cells.
- Only jet candidates of p_T harder than 20 GeV and in rapidity range $|\eta| < 2.8$ are retained.
- e^- (μ^-) are required to have $p_T > 7(6)$ GeV and in rapidity range$|\eta| < 2.47(2.7)$.
- Tau have not been considered here. We consider only e^- and μ^- as leptons in our analysis.
- To avoid double counting and miss-counting, After identifying jets and leptons, any jet within $\Delta\mathrm{R} < 0.2$ of a e^- (μ^-) is discarded.

- If e^-, μ^- and jet found within $\Delta\mathrm{R} < \min(0.4, 0.04 + \frac{10\mathrm{GeV}}{\mathrm{p_T^{e/\mu}}})$, e^- and μ^- discarded and it is recognized as a jet.
- Photon condidates are required to have $p_T > 25$ GeV and $|\eta| < 2.37$ excluding the transition region $1.37 < |\eta| < 1.52$ between the barrel and endcap electro-magnetic (EM) calorimeters.
- Any jet candidate lying within $\Delta\mathrm{R} < 0.4$ of a photon candidate has been discarded. Similarily, any photon candidate lying within $\Delta\mathrm{R} < 0.4$ of a e^-, (μ^-) candidate has been discarded.
- The missing transverse momentum vector p_T^{miss} (with magnitude E_T) is the sum of the calibrated transverse momentum of all e^-s, (μ^-)s, jets, photons candidates and all tracks originating from the primary vertex and that have not been taken into account for any other reconstructed object.
- Aplanarity is defined as 1.5 times to the lowest eigen value of the normalized momentum tensor of the jets.
- H_T has been taken as the scalar sum of p_T's of all the jets candidates of having p_T hardness more than 50 GeV and in rapidity range $|\eta| < 2.8$.
- $\mathrm{m_{eff}}$ is the sum of H_T and missing transverse energy E_T.
- In this whole analysis, jets with more than 50 GeV p_T hardness considered only.

Selection Cuts and Simulation Implementaion

- We have generated events at the MadGraph5aMC@NLO.2.6.5 and passed it to PYTHIA8.2.4.3 for hadronization of events
- To merge different parton level events, the CKKW − L merging scheme utilized.
- We implemented event reconstruction and detector level cuts in our designed code at Pythia
- FastJet.3.3.2 have been used for jet reconstruction.
- After reconstruction, all events filter out through pre-selection cut:

Lepton veto	No electron (muon)with $p_T > 7(6)$ GeV
E_T[GeV]	> 300
$p_T(j1)$ [GeV]	> 200
$p_T(j2)$ [GeV]	> 50
$\Delta\phi(j_{1,2,(3)}, p_T^{miss})_{min} >$[rad.]	> 0.4
m_{eff} [GeV]	> 800

- After preselection cuts, events pass to different signal region specific cuts:

Cut	SR2J-1600	SR2J-2200	SR2J-2800	SR4J-1000	SR4J-2200	SR4J-3400
$N_j \geq$	2	2	2	4	4	4
$\Delta\phi(j_{1,2,(3)}, E_T)_{min} >$	0.8	0.4	0.8	0.4	0.4	0.4
$\Delta\phi(j_{i>3}, E_T)_{min} >$	0.4	0.2	0.4	0.2	0.2	0.2
$p_T(j_1) >$[GeV]	250	600	250	100	100	100
$p_T(j_2) >$[GeV]	250	-	250	100	100	100
$p_T(j_3) >$[GeV]	-	-	-	100	100	100
$p_T(j_4) >$[GeV]	-	-	-	100	100	100
$\|\eta(j_{1,..,N_j})\| <$	2.0	-	1.2	2.0	2.0	2.0
Aplanarity $>$	-	-	-	0.04	0.04	0.04
$\frac{E_T}{\sqrt{H_T}} > [\sqrt{\text{GeV}}]$	16	16	16	16	16	10
$m_{eff} >$ [GeV]	1600	2200	2800	1000	2200	3400
$< \epsilon\sigma >^{95}_{obs}$[fb]	1.46	0.78	0.13	0.54	0.14	0.04

Cut	SR5J-1600	SR6J-1000	SR6J-2200	SR6J-3400
$\mathrm{N_j} \geq$	5	6	6	6
$\Delta\phi(j_{1,2,(3)}, E_T)_{min} >$	0.4	0.4	0.4	0.4
$\Delta\phi(j_{i>3}, E_T)_{min} >$	0.2	0.2	0.2	0.2
$p_T(j_1) >$[GeV]	600	-	-	-
$p_T(j_6) >$[GeV]	-	75	75	75
$\lvert\eta(j_{1,..,\mathrm{N_j}})\rvert <$	-	2.0	2.0	2.0
Aplanarity $>$	-	0.08	0.08	0.08
$\frac{E_T}{\sqrt{\mathrm{H_T}}} > [\sqrt{\mathrm{GeV}}]$	-	16	16	10
$\mathrm{m_{eff}} >$[GeV]	1600	1000	2200	3400
$< \epsilon\sigma >^{95}_{obs}$[fb]	0.36	0.11	0.04	0.02

- To validate our simulation implementation, we compared with provided result from the ATLAS search data.
- Cut flow chart for signal region SR4J-1000 :

Process	SUSY GG (direct) $m(\tilde{g}) = 2200$ GeV $m(\tilde{\chi}^0_1) = 600$ GeV	
Cuts	Absolute efficiency in%	
	the ATLAS	Our simulation
preselection$+\mathrm{N_j} \geq$2	100.0	99.9
$\mathrm{N_j} \geq$4	92.9	93.7
$\Delta\phi(j_{1,2,(3)}, E_T)_{min} > 0.4$	77.6	74.7
$\Delta\phi(j_{i>3}, E_T)_{min} > 0.2$	69.1	64.0
$p_T(j_4) > 100$ [GeV]	61.3	55.7
$\lvert\eta(j_{1,..,4})\rvert < 2.0$	55.7	50.2
Aplanarity > 0.04	38.7	33.5
$\frac{E_T}{\sqrt{H_T}} > 16[\sqrt{\mathrm{GeV}}]$	24.1	17.9
$\mathrm{m_{eff}} > 1000$[GeV]	24.1	17.9

Status of minimal-UED at Colliders

- For minimal UED scenario, level-1 KK particles have been pair produced and decayed to the SM and the LKP.
- After analysing the concerned signal regions, bound on the mUED parameters space consisting of cut-off scale of new physics Λ and compactification radius parameter R have been imposed.
- This is a 95% exclusion bound on R^{-1}-$\Lambda\mathrm{R}$ plane for different multi-jet signal regions of ATLAS [ATLAS-conf-2019-040] search in minimal UED.
- Thick black solid line shows the observed dark matter relic-density at present $\Omega_{DM}\mathrm{h}^2$ with a 3σ significance band, where Ω_{DM} is dark matter relic density and h is the Hubble constant at present.

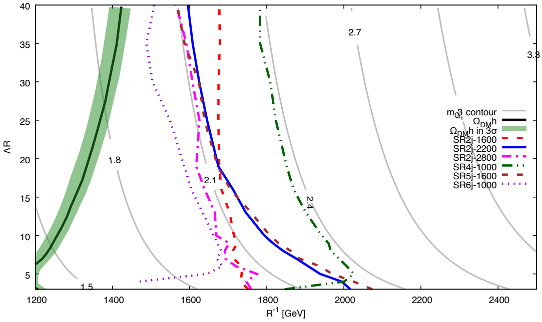

- Level-1 KK gluino mass (m_{G1}) contours have been depicted as grey lines along with corresponding mass values in TeV.
- The whole region right to the $\Omega_{DM}\mathrm{h}^2$ curve has been ruled out from the dark-matter searches:

Jonathan M. Cornell, Stefano Profumo, William Shepherd
Phys. Rev. D 89, 056005 (2014).

- The whole region left to respective signal region exclusion curves (e.g SR2J-1600) are ruled out from the ATLAS search ATLAS-conf-2019-040 at 95% confidence level.
- Combining both, there is no viable parameter space left for mUED scenario regarding to these signatures.
- We have to look into the non-minimal UED (nmUED) scenario for these signatures.

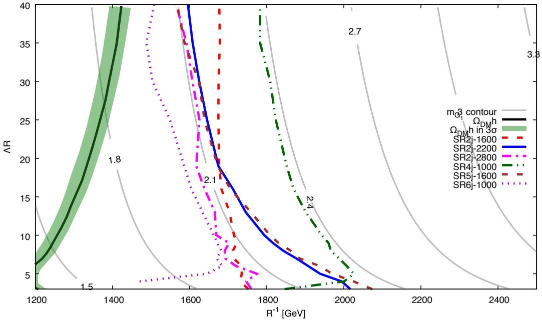

nmUED: BenchMark Points and Decay Profile

- The BLKT parameters must be greater than -π due to absence of any tachyonic state.
- There are some bounds available on the BLKT parameters from the LHC searches:

  T. Flacke, D. W. Kang, K. Kong, G. Mohlabeng, and S. C. Park
  JHEP 04 (2017) 041, [arXiv:1702.02949].

- For $R_B = 0$, any positive value of R_Q and R_G is forbidden as it gives rise to a stable colored particle.
- BPs are characterized by the R^{-1}, R_Q and R_G.
- We have assumed fiexd values: $R_L =$ -0.01, $R_\Phi = R_W =$ -0.02, $R_B = 0.0$.
- These choices make LKP mainly $B^{(1)}$ with a sufficient mixing with $W^{3(1)}$.

BPs	R^{-1} [TeV]	(R_Q, R_G)	$m_{G^{(1)}}$ [TeV]	$m_{Q^{(1)}}$ [TeV]	$m_{W^{(1)}}$ [TeV]	$m_{Z^{(1)}}$ [TeV]	$m_{L^{(1)}}$ [TeV]	$m_{B^{(1)}}$ [TeV]
BP_1^{nm}	1.9	(-0.9,-0.1)	1.963	2.559	1.913	1.914	1.906	1.900
BP_2^{nm}	2.1	(-0.1,-0.1)	2.169	2.169	2.114	2.115	2.107	2.100
BP_3^{nm}	2.0	(-0.3,-0.7)	2.531	2.209	2.013	2.015	2.007	2.000

BP 1: (R_Q, R_G)= (-0.9,-0.1), $m_{G^{(1)}} < m_{Q^{(1)}}$

- $Q^{(1)}$ primarily decays to a SM quark and $G^{(1)}$.
- $G^{(1)}$ decays to a SM quark - antiquark pair in association to $W^{(1)\pm}/Z^{(1)}/B^{(1)}$.
- Level 1 KK gauge boson subsequently decay to LKP and SM lepton. These leptons are very soft and will be accounted in missing E_T.

BP 2: (R_Q, R_G)= (-0.1,-0.1), $m_{G^{(1)}} = m_{Q^{(1)}}$

- $G^{(1)}$ primarily decays via 3 body decay to a SM quark-anti quark pair and the LKP.
- Level 1 KK quarks decay to the LKP and SM quarks
- These will give very soft jets

BP 3: (R_Q, R_G)= (-0.3,-0.7), $m_{G^{(1)}} > m_{Q^{(1)}}$

- $G^{(1)}$ primarily decays to a SM quark and level-1 KK counterpart.
- Level 1 KK doublet quark decays to a SM quark with $W^{(1)\pm}/Z^{(1)}/B^{(1)}$
- For level 1 KK singlet quark, decay BR to a SM quark and $W^{(1)\pm}$ is highly suppressed.

- Vissible cross-sections in different signal regions shown for R^{-1}= 1.8 TeV.
- The reddish cells depict higher value than the observed one at the ATLAS and are excluded in the respective signal region.
- SR2j-1.6 and SR2j-2.2 are more effective to probe the low and high R_Q regions.
- For high value of R_Q and R_G (BP_2^{nm}), gives too soft jet candidates to pass jet selection crietreia due to degenrate mass spectrum.
- The production of $G^{(1)}$ and $Q^{(1)}$ in association of ISR jet gives mono-jet $+E_T$ signal.
- SR2j-2.2 is basically mono-jet like signal, so it is effective to probe this part of plot.
- For low R_Q and/or low R_G (BP_1^{nm} and BP_3^{nm}), $G^{(1)}$ and $Q^{(1)}$ give hard jets due to higher mass than the LKP.

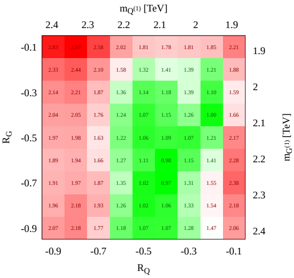

$\sigma_{SR2j-1.6}$ [fb] for R^{-1}=1.8 TeV

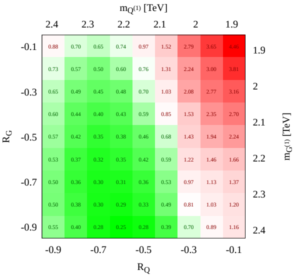

$\sigma_{SR2j-2.2}$ [fb] for R^{-1}=1.8 TeV

- The pair production of $G^{(1)}$ and $Q^{(1)}$ give 4 and 2 hard jets at the parton level, so SR2j-1.6 and SR4j-1.0 are more efficient to probe these parts.
- SR4j-1.0 is more effective to probe the intermidiate R_Q regions.
- We can see the complementarity of different signal regions.
- All the parts of R_Q-R_G plane has been ruled out with complementarity of different signal regions for R^{-1}= 1.8 TeV.

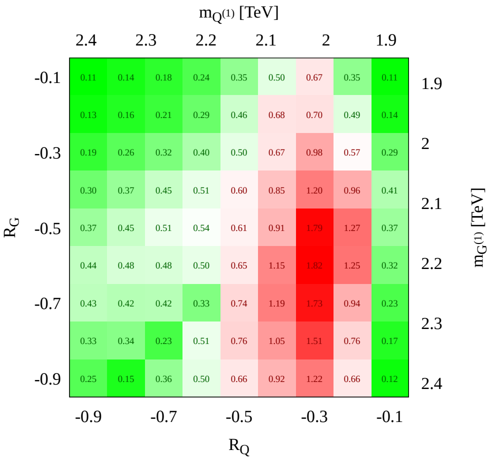

$\sigma_{SR4j\text{-}1.0}$ [fb] for R^{-1}=1.8 TeV

- The ATLAS multijet search can probe only some part of R_Q-R_G plane for R^{-1}= 1.9 TeV.
- Increased value of R^{-1} increases the overall mass scale of all the KK particles.
- This increment in the value of mass makes them safe from being excluded by the ATLAS multijet search.

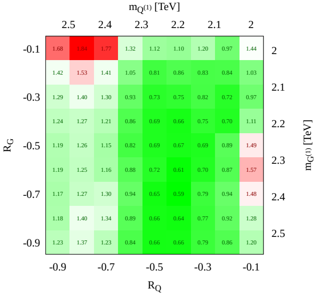

$\sigma_{SR2j-1.6}$ [fb] for R^{-1}=1.9 TeV

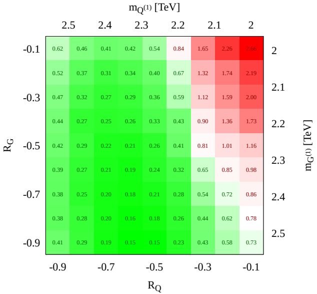

$\sigma_{SR2j-2.2}$ [fb] for R^{-1}=1.9 TeV

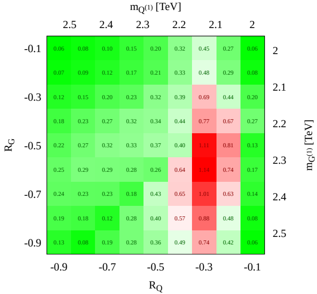

$\sigma_{SR4j-1.0}$ [fb] for R^{-1}=1.9 TeV

- We show the values of R^{-1} which have been ruled out by multijet signatures for nmUED parameters.
- We have taken $\mathrm{R_W}$= -0.02, $\mathrm{R_B}$ = 0.0, R_ϕ = -0.02, $\mathrm{R_L}$ = -0.01 for this plot.
- Values of ruled out R^{-1} with corresponding $\mathrm{R_G}$, $\mathrm{R_Q}$ shown along the respective multi-jet signal region.
- The Most of the regions have been ruled out by 2-jet and 4-jet signal region with different m_{eff} values(e.g. SR2j-1.6⇒ 1600 GeV).
- Max R^{-1} = 2.15 TeV has been ruled out in our scan for the highest values of $\mathrm{R_Q}$, $\mathrm{R_G}$ (-0.1,-0.1) from SR2j-2.2.
- The low bounds on R^{-1} can be 1.79 TeV for $\mathrm{R_Q}$, $\mathrm{R_G}$ (-0.5,-0.3) from SR4j-1.0.

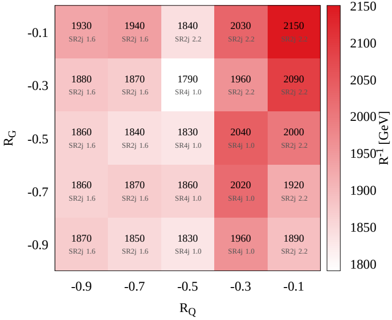

Conclusion

- In order to explain the inadequacies of the SM, UED frame work in **5 D** with one compact spatial dimension has been explored.
- We have utilised the ideas of dimension compactification and orbifolding to inculcate chiral fermions.
- mUED has been ruled out completely from collider and dark matter searches.
- We have explored the collider phenomenology of the Level 1 KK quark and gluon in nmUED scenario at the LHC.
- Exclusion bound on the BLKT parameters and radius of compactification have been placed from the multi-jet collider searches at the LHC.
- The dark matter phenomenology and other collider phenomenology parts are open for further exploration.
- This work will serve as a basis for further study of nmUED at the collider and DM searches.

arXive: 2012.15137